25th ABCM International Congress of Mechanical Engineering
October 20-25, 2019, Uberlândia, MG, Brazil

COBEM2019-0209
AN EFFICIENT FORMULATION FOR COUPLED GEOMECHANICS SIMULATIONS IN NONPAY-PAY REGIONS

Felipe W. Giacomelli
Hermínio T. Honório
António Fábio Carvalho da Silva
Clovis R. Maliska
Universidade Federal de Santa Catarina
felipe.g@sinmec.ufsc.br
herminio@sinmec.ufsc.br
afabio@sinmec.ufsc.br
maliska@sinmec.ufsc.br

Abstract. *This work proposes an efficient formulation for solving coupled geomechanics-flow in non permeable regions. The idea is to solve the mass conservation equation implicitly in the linear system only in the region containing the reservoir. Outside the reservoir, where the rock is impermeable, the fluid does not move so the mass conservation equation can be removed from the linear system and substituted into the geomechanical model, thus reducing the linear system size. The traditional way is to solve mass balance outside the reservoir and setting the permeability to zero, but this approach leans towards inefficiency, specially because the impermeable regions are usually bigger than the permeable ones. The results presented here show that the proposed formulations is consistent with the traditional. Additionally, the proposed formulation outperform the traditional approach in terms of CPU time up to 25%.*

Keywords: *poroelasticity, geomechanics, finite volume method*

1. INTRODUCTION

In reservoir simulations, when the geomechanical effects are not negligible, the computational domain is often composed of two different regions: the nonpay region (Ω_n) and the pay region (Ω_p), according to Fig. 1. The nonpay region encompasses a large zone outside the reservoir that is also affected by geomechanical effects, even though there is no fluid flow. This region is usually stiffer and has negligible permeability. The reservoir, referred to as the pay region due to its economic value, is composed of a permeable and softer material. The pay region is where the fluid flow takes place and it is also affected by geomechanics of the nonpay region.

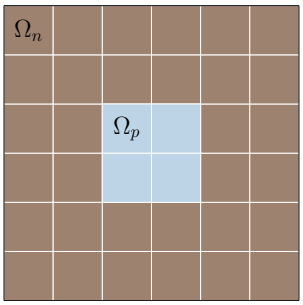

Figure 1. The pay region Ω_p is shown in blue, as the nonpay region Ω_n is depicted in brown.

Geomechanics and fluid flow in deforming porous media are governed by the equilibrium (momentum) equations and the mass balance equation. A force unbalance in a small region, such as Ω_p, affects the system as a whole ($\Omega_n + \Omega_p$), while fluid flow only takes place in permeable regions. Hence, the mass conservation equation can be solved only inside the pay region.

The approach traditionally employed in these situations is to solve the mass conservation equation in the whole com-

putational domain, setting a zero permeability throughout the nonpay region. The obvious drawback of this approach is that the mass balance equation is solved in the nonpay region, where there is no fluid flow. This procedure becomes more inefficient as Ω_n gets bigger than Ω_p.

For single-phase flows, the mass conservation equation provides only one algebraic equation for each control volume of the grid. However, for a two-phase flow model, two mass conservation equations are computed for each nodal point, so the traditional procedure of solving the fluid flow in the nonpay region implies in a unnecessary and even more significant computational effort. Since the solution of the resulting system of equations accounts, in general, for up to 70% of the total simulation time (Maliska, 2004), the possibility of reducing the number of equations to be solved is quite attractive. Less computational resources would be required in order to run the simulation, besides providing a significant speedup.

All these drawbacks may be avoided by properly managing the governing equations in the pay and nonpay domains. As sequential methods are employed to handle the coupling of fluid flow and geomechanics (Kim *et al.*, 2011), this management becomes more natural in comparison to the fully implicit coupling approach. Nevertheless, a simple way of doing so shall be proposed in this paper.

In what follows, both traditional and proposed mathematical formulations are presented in Sec. 2. In the sequence, Section 3 introduces the numerical method employed for discretizing the governing equations. In Section 4, three test cases are considered with the purpose of validating both formulations and to highlight the benefits of the proposed formulation in terms of CPU time savings. Finally, a few remarks close the presentation.

2. MATHEMATICAL MODEL

The equilibrium equations, considering the effective stress principle of Terzaghi (Terzaghi, 1923), can be written as follows,

$$\nabla_s^T(\mathbb{C}\nabla_s\mathbf{u} - \alpha p\mathbf{i}) \;=\; 0, \tag{1}$$

in which ∇_s is the symmetric nabla operator, $\mathbf{u}$ is the displacement vector, α is the Biot's coefficient, p is the pore pressure and $\mathbf{i}$ is a second order indentity tensor in Voigt notation. Finally, the constitutive matrix for linear elasticity, according to Hooke's law, can be represented as,

$$\mathbb{C} = \begin{bmatrix} 2G+\lambda & \lambda & \lambda & 0 & 0 & 0 \\ \lambda & 2G+\lambda & \lambda & 0 & 0 & 0 \\ \lambda & \lambda & 2G+\lambda & 0 & 0 & 0 \\ 0 & 0 & 0 & G & 0 & 0 \\ 0 & 0 & 0 & 0 & G & 0 \\ 0 & 0 & 0 & 0 & 0 & G \end{bmatrix}, \tag{2}$$

with G being shear modulus and λ denoting the first Lamè's parameter.

The single-phase fluid flow is modeled by the mass balance equation for deforming porous media in conjunction with Darcy's law. This model is referred to as Biot's consolidation model and it can be expressed as,

$$\frac{1}{M}\frac{\partial p}{\partial t} - \vec{\nabla}\cdot\left(\frac{\mathbf{k}}{\mu}\cdot\vec{\nabla}p\right) \;=\; -\alpha\frac{\partial \epsilon_v}{\partial t}, \tag{3}$$

in which the gravitational terms have been neglected. In Eq. 3, $\mathbf{k}$ represents the absolute permeability, μ is the fluid viscosity and ϵ_v denotes the volumetric strain ($\epsilon_v = \vec{\nabla}\cdot\mathbf{u}$). By its turn, M contains the Biot's modulus, defined by

$$M = [\phi c_f + (\alpha - \phi)c_s]^{-1}, \tag{4}$$

where ϕ, c_f and c_s stand for porosity, compressibility of the fluid and solid phases, respectively. It is important to note that if the tensor $\mathbf{k}$ equals to 0, the Darcy's velocity would also be 0, so there would be no fluid flow. For this reason, the traditional approach to reservoir simulation consists of setting null values to nonpay's permeability. Likewise, the same behavior could be achieved by setting a very large viscosity to the fluid in the nonpay region.

2.1 The proposed approach

The proposed formulation consists of implicitly solving the mass conservation equation only where fluid flow takes place, that is, in the pay region. Since the absolute permeability is zero in the nonpay region, the mass conservation equation, Eq. 3, reduces to

$$\frac{1}{M}\frac{\partial p}{\partial t} \;=\; -\alpha\frac{\partial \epsilon_v}{\partial t}. \tag{5}$$

A time integration of Eq. 5 leads to

$$p \;=\; p^o - \alpha M(\epsilon_v - \epsilon_v^o) \tag{6}$$

where p^0 and ϵ^0 denote pressure and volumetric strain evaluated at the previous time step. Therefore, in the nonpay region, the pore pressure is no longer an unknown and it can be determined by Eq. 6. Substituting Eq. 6 into Eq. 1 results in

$$\nabla_s^T(\mathbb{C}\nabla_s \boldsymbol{u} + \alpha^2 M\epsilon_v \mathbf{i}) \;=\; \nabla_s^T\left[(\alpha p^o + \alpha^2 M\epsilon_v^o)\mathbf{i}\right]. \tag{7}$$

It is important to notice that the mass balance equation cannot just be disregarded from the nonpay region, as if there was no fluid filling its pores. In fact, the pore fluid supports part of the external load and it has to be included in the geomechanical model. Thus, Eq. 1 and Eq. 3 shall be solved in the linear system only for the control volumes belonging to the pay region (Ω_p), while Eq. 7 is solved exclusively for the control volumes located outside the reservoir, in the nonpay region (Ω_n). Consequently, the dimensions of the resulting system of equations are appreciably reduced.

3. NUMERICAL FORMULATION

The Element-based Finite Volume Method (EbFVM) is used to obtain the algebraic form of Eq. 1, Eq. 3 and Eq. 7. This method ensures mass and momentum conservation for each control volume of the grid, thus rendering a fully conservative method. Additionally, it is naturally applied to unstructured grids composed of different types of elements, which provides substantial geometrical flexibility for discretizing complex regions.

As a cell-vertex method, in the EbFVM the control volumes are built around the grids vertices. As shown in Fig. 2, each element is subdivided into sub-elements associated to each element vertex. The union of all sub-element that share a common vertex composes a control volume. Furthermore, a control surface Γ_i bounds each control volume Ω_i. The faces of these surfaces are identified by an integration point, ip, on its midpoint, and an area vector, s, pointing outwards Ω_i.

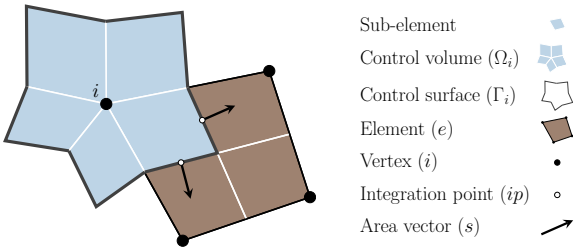

Figure 2. Geometrical entities for a bidimensional grid.

The algebraic equations corresponding to Eq. 1 and Eq. 3, are obtained through the EbFVM, as shown in (Honório *et al.*, 2018). Respectively, they read as

$$\sum_{ip\,\in\,\Gamma_i} \left[-K_{ip}\mathbf{u}^e + L_{ip}\mathbf{p}^e\right] = \mathbf{b}_i^u, \tag{8}$$

$$\sum_{ip\,\in\,\Gamma_i} \left[Q_{ip}\mathbf{u}^e - H_{ip}\mathbf{p}^e\right] + \frac{\Delta\Omega_i}{M\Delta t}p_i = \frac{\Delta\Omega_i}{M\Delta t}p_i^o + \sum_{ip\,\in\,\Gamma_i}\left[Q_{ip}(\mathbf{u}^e)^o\right] + \mathbf{b}_i^p, \tag{9}$$

with the matrices K_{ip} and L_{ip} accounting for the effective stresses and the pore pressures, respectively, in the stress equilibrium equations. Similarly, matrices H_{ip} and Q_{ip} account for, in that order, the Darcy velocities and the solid velocities (volumetric strain) in the mass conservation equation. Also, it is important to recall that the superscript "o" (old) indicates variables computed in the preceding time step.

If those algebraic equations are assembled for every grids vertex, as usually, the corresponding linear systems for a simultaneous solution, they will read

$$\begin{bmatrix} -K & L \\ Q & A-H \end{bmatrix}_{4N\times 4N} \begin{bmatrix} \mathbf{u} \\ p \end{bmatrix}_{4N\times 1} = \begin{bmatrix} b^{\mathbf{u}} \\ b^p \end{bmatrix}_{4N\times 1}, \tag{10}$$

in which A is a diagonal matrix containing the coefficients related to the accumulation term, and N denotes the number of control volumes of the grid ($\Omega_n + \Omega_p$).

3.1 The proposed formulation

Following the same procedure described in the beginning of this section, the algebraic equation associated to Eq. 7 may be written as

$$\sum_{ip \in \Gamma_i} (-K_{ip} + D_{ip})\mathbf{u}^e = \sum_{ip \in \Gamma_i} [D_{ip}(\mathbf{u}^e)^o + L_{ip}(\mathbf{p}^e)^o] + \mathbf{b}_i^u, \tag{11}$$

where matrix D_{ip} represents the divergence operator, responsible for computing the volumetric strain ϵ_v. The assembly of Eq. 11 results

$$\begin{bmatrix} -K+D & -K & 0 \\ -K & -K & L \\ Q & Q & A-H \end{bmatrix}_{3N+N_p \times 3N+N_p} \begin{bmatrix} \mathbf{u}_n \\ \mathbf{u}_p \\ p_p \end{bmatrix}_{3N+N_p \times 1} = \begin{bmatrix} b^{\mathbf{u}_n} \\ b^{\mathbf{u}_p} \\ b^{p_p} \end{bmatrix}_{3N+N_p \times 1}, \tag{12}$$

where N_p represents the number of control volumes in the pay region Ω_p.

The linear system size reduction is proportional to the ratio between the number of control volumes in the pay region (N_p) and the nonpay region (N_n). Considering that the nonpermeable domain must be sufficiently large ($\Omega_n >> \Omega_p$) in order to justify the zero displacement boundary conditions, a substantial amount of equations may be eliminated from the linear system.

In addition, it is necessary to recall that Eq. 6 is employed for the evaluation of pressure outside the pay region, since these values are required in Eq. 11. Moreover, the fluid pressure plays an important role in the overall structure of the domain, as it also supports external load.

4. RESULTS

Regarding the software implementation, an in-house C++ library named *EFVLib2018* was particularly developed to offer geometrical support for EbFVM applications. The *Portable, Extensible Toolkit for Scientific Computation* (Abhyankar *et al.*, 2018) was employed for preconditioning and solving the linear systems. Also, the input of the grids and the output of numerical fields was done through *MSHtoCGNS* (Giacomelli, 2018). Finally, all plots shown in this section were crafted with the aid of *Matplotlib* (Hunter, 2007).

The purpose of the test cases presented in this section is threefold. First, the two-layered poroelastic column with different nonzero permeabilities is employed to validate the implementation of the traditional methodology checking against the analytical solution. The proposed formulation was not compare with the analytical solution since the latter does accept zero permeability. Once the implementation of the traditional formulation is validated, it is used to validate the proposed formulation in a two-layered poroelastic column with a impermeable bottom layer. A performance analysis is realised in the second problem. Finally, a problem representing a reservoir depletion through a producing well is solved with both formulations. The reservoir is entrapped by two impermeable layers. In this problem we show that both formulations provide exactly the same solution, pointing out the benefits of the proposed formulation for representing the nonpay region.

4.1 Two layers poroelastic column - analytical solution

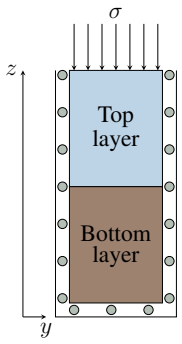

Figure 3. Two layers poroelastic column.

The first problem consists of a 1 m x 1 m x 6 m poroelastic column, as depicted in Fig. 3. All of its surfaces are sealed, except for the top draining boundary, where the pressure is prescribed equal to 0. In addition, all boundaries

have zero normal displacement, except for the top boundary, which has a constant compressive load $\sigma = 1.00 \times 10^7\ Pa$ applied. The fluid and poroelastic properties are displayed in Tab. 1 and Tab. 2, respectively.

Property	Unit	Water
μ	$Pa \cdot s$	1.00×10^{-3}
c_f	Pa^{-1}	3.03×10^{-10}

Table 1. Fluid properties.

Property	Unit	Top layer	Bottom layer
k	m^2	1.90×10^{-14}	1.90×10^{-15}
G	Pa	$6.00 \times 10^{+9}$	$6.00 \times 10^{+9}$
c_s	Pa^{-1}	2.77×10^{-11}	2.77×10^{-11}
α	–	7.78×10^{-1}	7.78×10^{-1}
ϕ	–	1.90×10^{-1}	1.90×10^{-1}

Table 2. Poroelastic properties.

The analytical solution for this problem is presented in details in (Verruijt, 2016). The numerical solution, obtained with the traditional formulation, is represented by Eq. 10. The tetrahedral grid has a total of 3612 control volumes and a time step size of $\Delta t = 0.5\ s$ has been employed. Figure 4 presents the analytical and numerical solutions of the pressure profile along the vertical direction z for different time levels. As can be verified, the pressure profile develops faster in the upper layer due to its higher permeability, what is perfectly captured by the numerical formulation.

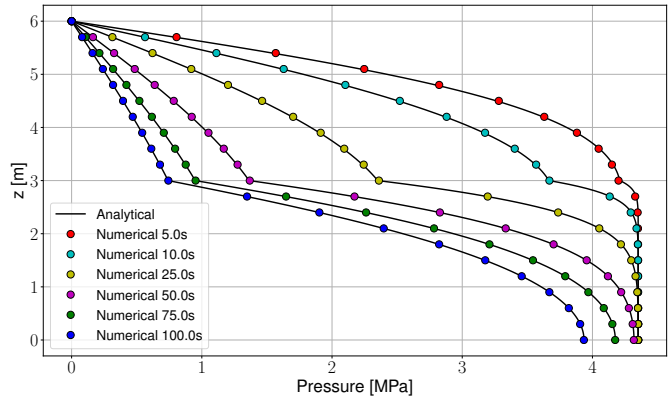

Figure 4. Pressure profile over time for the two layer poroelastic column.

4.2 Two layers poroelastic column - comparison between formulations

Setting the bottom layer permeability to zero, the proposed formulation may be tested against with the traditional one. For this problem, a grid composed of hexahedra with 3549 nodal points was employed for obtaining the results shown in Fig. 5. As it can be verified in this figure, the pressure and displacement profiles obtained with the traditional and the proposed formulation are exactly the same.

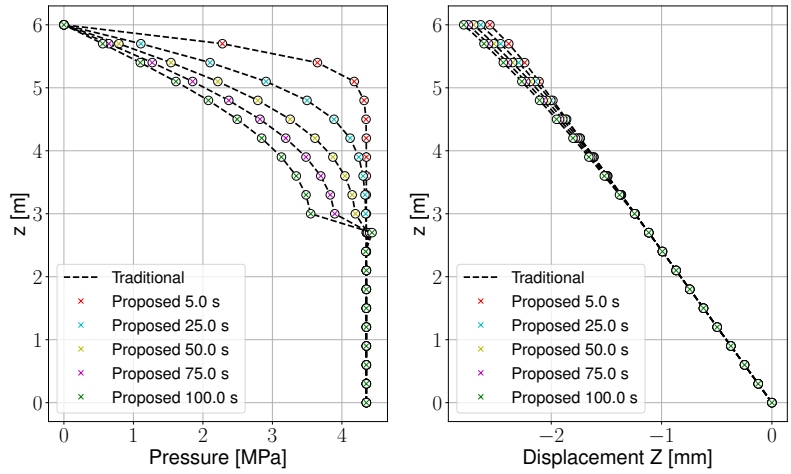

Figure 5. Comparison between results obtained through traditional and proposed formulations.

Still on this figure, it might be noticed small pressure instabilities in the interface between the two layers. In this region occurs an undrained consolidation process that gives rise to pressure instabilities when equal order approximations are employed for both pressure and displacement, according to the LBB-condition (Guzmán *et al.*, 2013). Although a stabilization technique has already been developed for the EbFVM, as seen in (Honório, 2018) and (Maliska and Honório, 2019), it has not been employed in the present work. For poroelasticity, however, these pressure wiggles tend to disappear as the solution progresses in time.

In this problem the top layer could be recognized as the pay region, Ω_p, since it has nonzero permeability, and the nonpay region Ω_n is represented by the bottom layer. The speedup provided by the proposed formulation will obviously depend on the number of control volumes in the pay region, N_p, and in the nonpay region, N_n. Thus, we define a ratio between these two quantities as

$$R = \frac{N_p}{N_n}. \tag{13}$$

In this manner, we analyze the performance of both formulations in terms of the ratio R. The smaller the value of R ($N_n > N_p$), the larger should be the expected speedup observed for the proposed formulation, since N_n mass balance equations are eliminated from the linear system. This behavior is shown in Fig. 6, where the larger speedup is observed for $R = 0.25$. This means that, when N_n is four times N_p, the proposed formulation can reduce the overall CPU time by about 25% comparing to the traditional one. When $R = 1.5$ the speedup is about 12%.

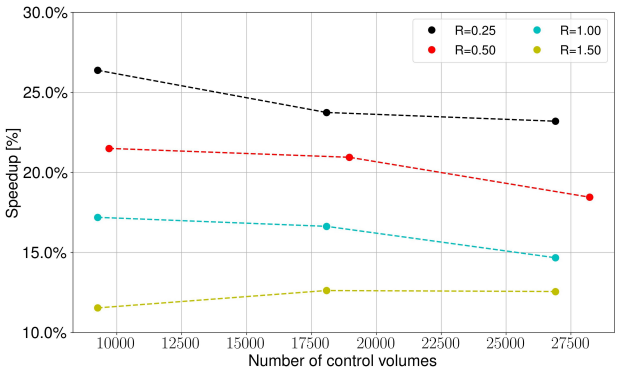

Figure 6. Speedup for grids with different ratios R.

The corresponding CPU time of the speedups depicted in Fig. 6 are shown in Fig. 7, the coupling between the fluid flow and geomechanical model was handled with the sequential method *Fixed-Stress* (Kim *et al.*, 2011). Grids with 9, 18 and 27 thousand control volumes, approximately, were employed. They were generated by the extrusion of an evenly spaced 21x21 Cartesian grid. Consequently, the grid refinement between them was performed only in z direction. Figure 7 shows the CPU time increasing with grid refinement for different ratios R. In accordance with the results shown in Fig. 6, a larger distance between the traditional and proposed formulations in Fig. 7 is verified for $R = 0.25$.

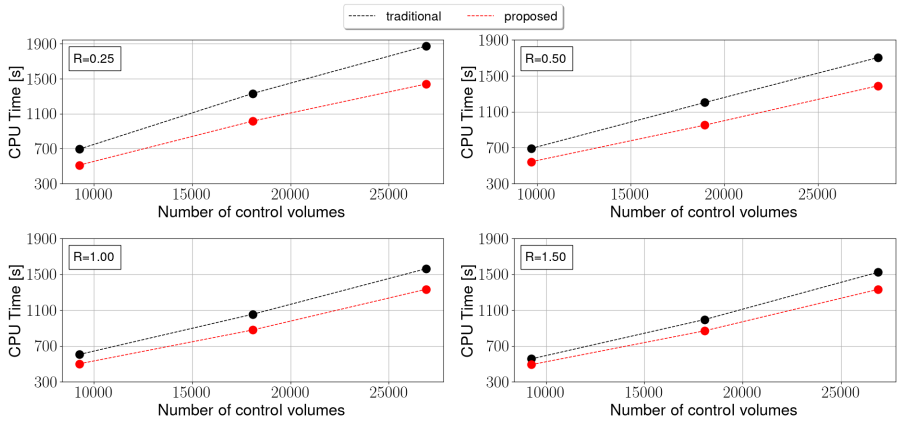

Figure 7. Comparison between CPU time spent by traditional and proposed formulations.

4.3 Reservoir depletion

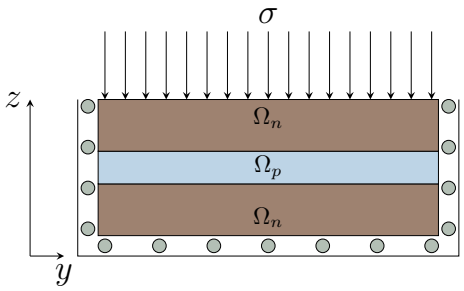

Figure 8. Domain sketch.

Property	Unit	Pay Ω_p	Nonpay Ω_n
k	m^2	1.90×10^{-15}	0.0
G	Pa	$6.00 \times 10^{+9}$	$6.00 \times 10^{+11}$
c_s	Pa^{-1}	0.0	0.0
α	–	1.0	1.0
ϕ	–	1.90×10^{-1}	1.90×10^{-1}

Table 3. Poroelastic properties.

In this scenario, a soft productive reservoir lays between two layers of stiff impermeable rock, as depicted in Fig. 4.3 The domain is bounded by a 10000 m x 6000 m x 1400 m box, where the first 600 m in the vertical direction accounts for the underburden, the next 200 m represents the pay region, and the last 600 m renders the overburden. The poroelastic properties of both regions are listed in Tab. 3, as the fluid properties are displayed on Tab. 1.

Initially, all the domain is stress-free and the fluid pressure equals to 0. The top boundary has a constant compressive load $\sigma = 1.00 \times 10^7\ Pa$ applied, while all other boundaries have zero normal displacement and are sealed. Also, a time step size of 5 days was used throughout the simulation.

In the center of the reservoir, a vertical well with a wellbore radius of 0.05 m is completed. It produces at a rate of $9.2 \times 10^{-2}\ m^3/s$ during the whole simulation. The Peaceman well model (Peaceman, 1978) is employed.

The pressure in a control volume located at coordinates (2500, 3000, 800), in the interface between the reservoir and the overburden, is shown in the left side of Fig. 9. It can be seen that the Mandel-Cryer effect (Mandel, 1953) may be observed, which is characterized by an increase in the reservoir pressure due to the undrained conditions happening close to the interface. This phenomenon is a clear indication of the coupling between fluid flow and geomechanics, and cannot be captured with uncoupled formulations.

By its turn, the right hand plot of Fig. 9 shows the pressure in a control volume located in the overburden, whose centroid is at (2500, 3000, 1100). Employing the proposed formulation, the pressure values in this position were obtained through Eq. 6. Again, both formulations provide exactly the same results, which reveals the consistency of the proposed formulation.

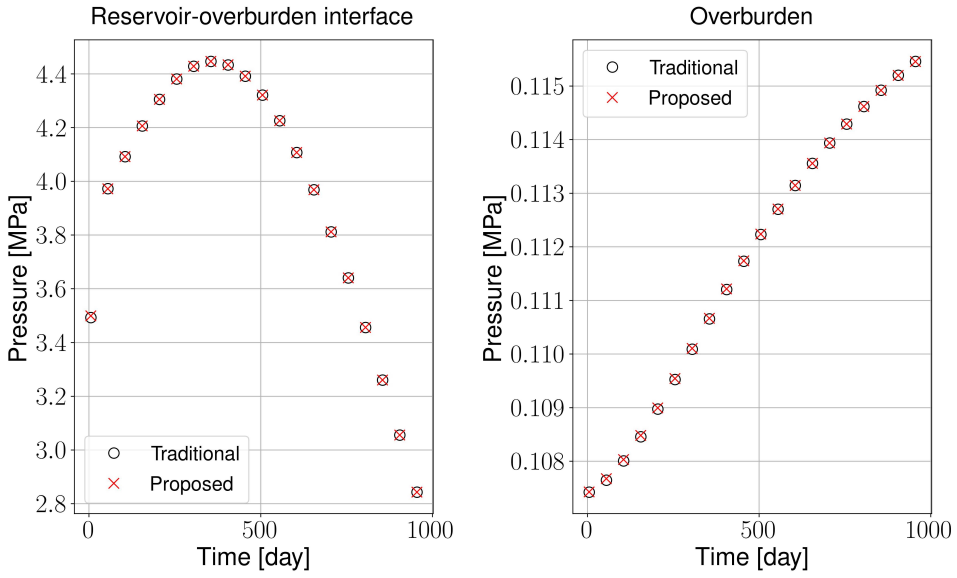

Figure 9. Comparison between pressure values obtained through traditional and proposed formulations.

In order to demonstrate the gain in perfomance of the proposed formulation when a simultaneous solution approach is used, both geomechanics and mass conservation equations were assembled and solved in a single linear system for the reservoir depletion problem. The CPU times, as well as the speedup, achieved for $R = 0.5$ are pictured in Fig. 10. This figure suggests that the proposed formulation becomes more attractive as the grid is refined.

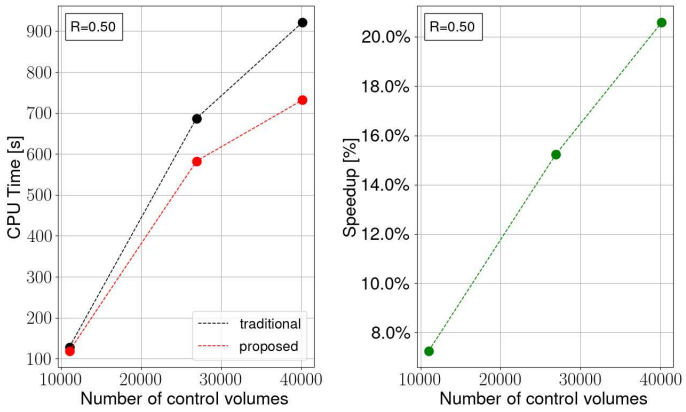

Figure 10. CPU time spent by traditional and proposed formulations and the reached speedup.

5. CONCLUSIONS

This paper discusses two different ways for treating the nonpay region surrounding a reservoir. The traditional approach for this problem is to set zero permeability for this region and to solve the mass balance equation implicitly in the linear system. The main goal of this work is to propose an alternative formulation for representing the nonpay region with the purpose of reducing the number of equations in the linear system, and thus reducing the CPU time. It is shown that the integration of the mass conservation equation in an impermeable medium provides a simple algebraic equation for pressure that can be included into geomechanical model, thus eliminating these equations from the linear system.

A comparison between the traditional and the proposed approach revealed that both of them the provide exactly the same results for all problems presented, which indicates the consistency of the proposed formulation. Additionally, a performance analysis has been carried out. It was shown that the proposed formulation outperformed the traditional one in all cases. The speedup provided by the proposed formulation increases when the number of control volumes in the nonpay region increases, as should be expected.

Moreover, the proposed formulation has been successfully applied with the sequential fixed-stress and the fully implicit coupling schemes. Although the implementation for the sequential scheme is far less complicated, the implementation for the fully implicit scheme is also manageable.

Finally, it should be noted that when multiphase fluid flow models are to be used, the speedup of the proposed formulation is expected to increase even more. This is justified because the mass conservation equation may yield not only more unknowns but also nonlinearities. Therefore, to solve this equation in only parts of the computational domain is an attractive feature for any reservoir simulator.

6. ACKNOWLEDGEMENTS

This paper has been partially funded by Petrobras within project number 11019, entitled "Malhas Tridimensionais Híbridas para a Solução do Problema Acoplado Fluxo-Geomecânica".

7. REFERENCES

Abhyankar, S., Brown, J., Constantinescu, E.M., Ghosh, D., Smith, B.F. and Zhang, H., 2018. "Petsc/ts: A modern scalable ode/dae solver library". *arXiv preprint arXiv:1806.01437*.

Giacomelli, F.W., 2018. "MSHtoCGNS: An Interface to Numerical Simulation I/O". *Computing in Science & Engineering*.

Guzmán, J., Salgado, A.J. and Sayas, F.J., 2013. "A note on the ladyženskaja-babuška-brezzi condition". *Journal of Scientific Computing*, Vol. 56, pp. 219–229.

Honório, H.T., 2018. *A Stabilization Technique For Treating Numerical Instabilities In Three-dimensional Poroelasticity*. Ph.D. thesis, Universidade Federal de Santa Catarina, Florianópolis, Brasil.

Honório, H.T., Giacomelli, F., da Silva, L.G.T. and Maliska, C.R., 2018. "A unified formulation for solving coupled geomechanics". In *Proceedings of the Rio Oil & Gas Expo and Conference 2018*. Rio de Janeiro, Brazil.

Hunter, J.D., 2007. "Matplotlib: A 2d graphics environment". *Computing in Science & Engineering*, Vol. 9, No. 3, pp. 90–95. doi:10.1109/MCSE.2007.55.

Kim, J., Tchelepi, H.A. and Juanes, R., 2011. "Stability and convergence of sequential methods for coupled flow and geomechanics: Fixed-stress and fixed-strain splits". *Computer Methods in Applied Mechanics and Engineering*, Vol.

200, p. 1591–1606.

Maliska, C.R., 2004. *Transferência de Calor e Mecânica dos Fluidos Computacional*. LTC Editora, Rio de Janjeiro, 2nd edition.

Maliska, C.R. and Honório, H.T., 2019. "ressure-displacement coupling in poroelasticity. further details of a stable finite volume formulation". In *VIII Conference on Computational Methods for Coupled Problems in Science and Engineering - COUPLED PROBLEMS 2019*. Sitges, Spain.

Mandel, J., 1953. "Consolidation des sols". *Géotechnique*, p. 287–299.

Peaceman, D.W., 1978. "Interpretation of well-block pressures in numerical reservoir simulation". *SPE Journal*, p. 183–194.

Terzaghi, K., 1923. "Die berechnung der durchlassigkeitsziffer des tones aus dem verlauf der hydrodynamischen spannungsercheinungen". Sitzung berichte. Akademie der Wissenschaften, Wien Mathematiesch-Naturwissenschaftliche Klasse.

Verruijt, A., 2016. *Theory and problems of poroelasticity*. Delft University of Technology, Netherlands.

8. RESPONSIBILITY NOTICE

The authors are the only responsible for the printed material included in this paper.